

The Autosomal Recessive Polycystic Kidney Disease Protein Is Localized to Primary Cilia, with Concentration in the Basal Body Area

SHIXUAN WANG,* YING LUO,* PATRICIA D. WILSON,[†]
GEORGE B. WITMAN,[‡] and JING ZHOU*

*Renal Division, Department of Medicine, Brigham and Women's Hospital and Harvard Medical School, Boston, Massachusetts; [†]Division of Nephrology, Department of Medicine, Mount Sinai School of Medicine, New York, New York; and [‡]Department of Cell Biology, University of Massachusetts Medical School, Worcester, Massachusetts.

Abstract. Recent evidence suggests that structural and functional abnormalities of primary cilia in kidney epithelia are associated with mouse and human autosomal dominant polycystic kidney disease. To determine whether fibrocystin/polyductin/tigmin (FPC), the protein product encoded by the *PKHD1* gene that is responsible for autosomal recessive polycystic kidney disease among human subjects, is also a component of primary cilia in the kidney, antipeptide antibodies to the carboxyl-terminal intracellular domain and amino-terminal extracellular domain of FPC were generated and were characterized with immunoblotting and immuno-light and -electron

microscopy. Immunolocalization in normal kidney tissue sections and cultured kidney cells demonstrated that FPC was localized to the primary cilia and concentrated on the basal bodies in both kidney tissue sections and cultured kidney cells. The FPC expression pattern was not altered in kidney cells with *Pkd1* mutations. These findings suggest that FPC is a functional and/or structural component of primary cilia in kidney tubular cells. It is proposed that the pathogenesis of autosomal recessive polycystic kidney disease is linked to the dysfunction of primary cilia.

Polycystic kidney diseases (PKD) are a large group of diseases characterized by the development of multiple fluid-filled cysts in the kidney, gradually leading to end-stage renal failure. Autosomal recessive PKD (ARPKD), also known as polycystic kidney and hepatic disease 1 (PKHD1) or infantile PKD type I, is one of the inherited kidney disorders found in infancy, with an estimated prevalence varying from one case/6000 newborns to one case/40,000 newborns (average of one case/20,000 newborns) (1,2). ARPKD presents in infancy as huge bilateral polycystic kidneys, oligohydramnios, and pulmonary hypoplasia; the latter complication is thought to be the major cause of death. With current improved treatment, mortality rates still reach 30% for infants with ARPKD (3–5). Approximately one-half of the children who survive the neonatal period develop end-stage renal failure (6). ARPKD is often accompanied by biliary dysgenesis, hepatic fibrosis, portal hypertension, and systemic hypertension (4,7,8). Cysts in the kidney arise

mainly from the collecting ducts, although transient cysts were observed in proximal tubules during kidney development (9,10).

ARPKD is caused by mutations in *PKHD1*. Sixty-three mutations have been identified to date, including frameshift, nonsense, missense, and out-of-frame splicing alterations (11–13). The longest isoform of the *PKHD1* transcripts among human subjects is 16,235 bp (12). Several shorter transcripts of *PKHD1* were also suggested (13,14). The open reading frame in the human gene is 12,222 bp, encoding a large 4074-amino acid protein with a calculated molecular mass of 447 kD, designated fibrocystin/polyductin/tigmin (FPC) (12–14). FPC was proposed to be a novel single-transmembrane protein with a short 192-amino acid carboxyl-terminal intracellular domain and a very large amino-terminal extracellular portion containing domains such as TIG, TIG-like, TMEM2, and DKFZ homologs and to belong to a protein superfamily with adhesive functions (12–14). The longest open reading frame of the mouse ortholog of *PKHD1* encodes a protein of 4059 amino acids; the mouse and human protein sequences are 73% identical overall and 55% identical in the carboxyl-terminal tail. Study of the expression pattern in mouse metanephros by *in situ* hybridization demonstrated that *Pkhd1* transcripts are not expressed in metanephric mesenchyme but are strongly expressed in the branching ureteric bud, which later develops into the adult collecting ducts (15,16). In postnatal kidney tissue, strong *Pkhd1* expression was observed in collecting ducts, with lower levels in proximal and distal tubules (15).

Received June 11, 2003. Accepted November 16, 2003.

Correspondence to Dr. Jing Zhou, Harvard Institutes of Medicine, Room 522, Brigham and Women's Hospital and Harvard Medical School, 4 Blackfan Circle, Boston, MA 02115. Phone: 617-525-5860; Fax: 617-525-5861; E-mail: zhou@rics.bwh.harvard.edu

1046-6673/1503-0592

Journal of the American Society of Nephrology

Copyright © 2004 by the American Society of Nephrology

DOI: 10.1097/01.ASN.0000113793.12558.1D

The primary cilium, which is found on many types of mammalian epithelial cells, is a specialized sensory organelle extending from the cell surface (17–19). It is assembled as an extension of a basal body, which itself originates from one of a pair of centrioles (20). In most kidney tubular epithelial cells except intercalated cells, a single primary cilium protrudes into the tubular lumen (21). The primary cilium in kidney tubules contains a central axoneme with a 9+0 arrangement of microtubules (22). IFT88/Polaris, the protein product encoded by *Tg737*, whose mutation causes PKD in mice, is localized in the peri-basal body region and primary cilium and is required for ciliogenesis in *Chlamydomonas* (23), in *Caenorhabditis elegans* (24), and in mice (23,25). Recent evidence demonstrated that cilia are able to sense fluid flow (26) and that this sensory process is mediated by polycystin 1 (PC1) and PC2, the proteins responsible for autosomal dominant PKD (27). Whether FPC is expressed and functions in cilia is not known. Therefore, as the first step in elucidating the pathogenesis of ARPKD, we generated two anti-peptide antibodies (803 and 804) against FPC and characterized them with immunoblotting and immuno-light microscopy and immuno-electron microscopy. We determined that FPC in kidney tubular cells is localized to the primary cilia, with concentration in the peri-basal body region.

Materials and Methods

DNA Constructs and Reagents

We amplified the most 3' 576-bp and 5' 648-bp coding sequences of *PKHD1* with reverse transcription-PCR and digested the fragments with *HindIII* and *XbaI*. *Taq* DNA polymerase was used for PCR after first-strand cDNA synthesis with SuperScript II RNase H reverse transcriptase, in the presence of oligo(dT)_{12–18} or *PKHD1*-specific primer (hPKHD1-RT2, 5'-CTGACCTGGTGATGGAAGAAATGGAAAAGA-3'). For PCR, the sequence-specific sense primers (hPKHD1-F7, 5'-TACGAAGCTTCCACCATGAAAAGAAGCAAAAGCAGAAAAACAAAACCTGAAGAG-3'; hPKHD1-Up5, 5'-ATCGAAGCTTCCACCATGTGGTCA-GAGGAACCAAGGACTAAGGTGAAA-3') and antisense primers (hPKHD1-R7, 5'-AGTCTCTAGAGCCAGTTGCTCC-TGAATAGTTTCCGGGTGTAC-3'; hPKHD1-Down5, 5'-AGTCTCTAGAGCGCCTTTGTATGCAAGACACAGGTGTGT-ATACTGATC-3') were designed according to the human FPC cDNA sequence (GenBank accession no. AY074797). The PCR amplification began with denaturation at 94°C for 5 min and continued with annealing and elongation at 68°C for 2 min, followed by 35 cycles. The DNA constructs were confirmed to be correct with DNA sequencing. All reagents except human RNA (Clontech Laboratories, Palo Alto, CA) were purchased from Invitrogen (San Diego, CA). The two constructs, named pcDNA4/hPKHD1CT and pcDNA4/hPKHD1NT, encoded the most carboxyl-terminal 192 amino acids and the amino-terminal 216 amino acids of FPC, respectively.

Generation and Purification of Polyclonal Antibodies against Human FPC

To generate antibodies against human FPC, we selected one peptide sequence located in the intracellular domain (amino acids 3912 to 3925, KRRESQGPKKEDTV) and one located in the extracellular domain (amino acids 488 to 502, REKHQIRVRAQLPE). Each

peptide was synthesized and injected into two rabbits (Research Genetics, Invitrogen). Antibodies from 10-wk blood samples were affinity-purified and designated 803 and 804.

Cell Culture and Transient Transfection

Human embryonic kidney (HEK) 293T cells were cultured in 1× Dulbecco's modified Eagle's medium (DMEM) (Life Technologies, Grand Island, NY) containing 10% FBS (Invitrogen) and were transiently transfected with FuGENE 6 transfection reagent (Roche, Welwyn Garden City, UK) after overnight culture, according to the manufacturer's instructions. *Dolichos biflorus* agglutinin (DBA)-positive mouse embryonic kidney (MEK) cells (*Pkd1*^{null/+}, *Pkd1*^{null/null}, and *Pkd1*^{del34/del34}) (28,29) were derived from embryonic day 15.5 kidneys from wild-type and *Pkd1* mutant mice bearing temperature-sensitive simian virus large T antigen (27). Cells were cultured at 33°C in SV40 epithelium medium, containing 1× DMEM, 5% FBS, 0.75 μg/L IFN-γ, 1 g/L insulin, 0.67 mg/L sodium selenite, 0.55 g/L transferrin, 0.2 g/L ethanolamine, 36 ng/ml hydrocortisone, 0.1 μM 2,3,5-triiodo-L-thyronine, 0.3 mg/ml glutamine, 0.1 mM citrate, and appropriate amounts of antibiotics. All of the cell culture supplements were obtained from Invitrogen except for IFN-γ, hydrocortisone, and 2,3,5-triiodo-L-thyronine (Sigma Chemical Co., St. Louis, MO). These cells have been passaged >50 times with no apparent phenotypic changes. Human kidney DBA-positive renal cortical tubule epithelial cells (30) were cultured in DMEM/15% FBS at 37°C; canine kidney MDCK cells were cultured in DMEM/10% FBS at 37°C. These studies were completely in compliance with human research guidelines, and institutional review board approval was obtained.

Western Blotting

Two days after transfection, cultured HEK 293T cells were harvested and solubilized with RIPA buffer (150 mM NaCl, 1% Nonidet P-40, 0.5% sodium deoxycholate, 0.1% SDS, 50 mM Tris, pH 7.6) containing appropriate proteinase inhibitors (complete EDTA-free tablets; Roche) and 10 mM PMSF. The cell lysates were frozen and thawed for three rounds before being passed through a 27-gauge syringe 10 times. Cells were then centrifuged at 10,000 × g for 10 min at +4°C. Twenty microliters of the supernatant were used for immunoblotting analysis.

The protein samples were subjected to electrophoresis in a 12% acrylamide Laemmli resolving gel (mini-gel electrophoresis system; Bio-Rad Laboratories, Richmond, CA) and transferred to Hybond ECL nitrocellulose membranes (Amersham Pharmacia Biotech, Piscataway, NJ). After being blocked with 5% nonfat dry milk (Bio-Rad Laboratories) in PBS for 1 h, the filter was incubated with rabbit antibody to FPC, with or without peptide, for another 1 h. After three washes with PBS/0.2% Tween 20 (Bio-Rad Laboratories), the filters were incubated with donkey anti-rabbit Ig conjugated with horseradish peroxidase-linked antibody (1:10,000; Amersham Biosciences). After thorough washing, the bound antibodies were detected with the ECL Western blotting analysis system (Amersham Pharmacia Biotech), according to the manufacturer's instructions. For Myc tag detection, the filter was stripped with Restore Western blot stripping buffer (Pierce Chemical Co., Rockford, IL), reblotted with mAb to Myc (1:5000; Invitrogen), and subjected to the procedures described above. For peptide blocking experiments, 803 and 804 were incubated with FPC peptides (200-fold molar excess) for at least 1 h at room temperature before being added to the filter.

Immuno-Light-Microscopic Analysis of Kidney Cells and Kidney Tissues

The methods for immunostaining in kidney cells and kidney tissues have been described in detail (27). In brief, cells were cultured as described above for at least 2 d (to approximate subconfluence), fixed with 3% paraformaldehyde/2% sucrose, and permeabilized with 0.5% Triton X-100 (Sigma). Permeabilized cells were incubated with the antibody against FPC (1:250 for 803 and 804) for 1 h at room temperature and then with the FITC-labeled goat anti-rabbit mAb (1:1000). For double-labeling, the antibody against FPC and mAb to acetylated α -tubulin or γ -tubulin (1:10,000) were concomitantly incubated. After thorough washing, both Texas Red-labeled (1:1000) and FITC-labeled secondary antibodies (1:1000) were added for 1 h at room temperature. Before mounting with Prolong antifade medium (Molecular Probes, Eugene, OR), the cells were incubated for 5 min with 4'-6-diamidino-2-phenylindole (1:5000 in 1 \times PBS). For tissue staining, human and mouse kidney tissues were fixed with 4% paraformaldehyde for 24 h and then transferred overnight to 30% sucrose in 0.2 M phosphate buffer containing Na₂HPO₄ and NaH₂PO₄. The tissues were embedded in Tissue-Tek OCT compound (Sakura Finetek USA, Torrance, CA), sectioned at 5 to 7 μ m, and fixed in acetone at -20°C for 5 min. Other procedures for staining of the kidney tissue were the same as for the cells except without Triton X-100. A Zeiss Axioskop2 Plus fluorescence microscope (Carl Zeiss, Inc., Thornburg, NY) was used to observe the signal, and the Spot camera system (Diagnostic Instruments) was used for photography.

Immunoprecipitation of Endogenous FPC with 803 and 804

DBA-positive renal cortical tubule epithelial cells and MDCK cells were harvested and solubilized as described above for HEK 293T cells. Normal human kidney samples were homogenized in RIPA buffer with a mortar and pestle and then a tissue homogenizer. Cell lysates and tissue homogenates were centrifuged at 10,000 \times g for 20 min at +4°C. The supernatants were precleared with protein A-agarose beads (Invitrogen) for 1 h at +4°C before the addition of 803 or 804. After endogenous FPC was immunoprecipitated overnight, protein A-agarose beads were added and incubated at +4°C for 3 h, followed by centrifugation at 10,000 \times g for 1 min at +4°C. The beads were washed twice with RIPA lysis buffer. Finally, 50 μ l of sample buffer was added and the samples were analyzed with Western blotting. The procedures were the same as described above except that the samples were electrophoresed on a 5% acrylamide Laemmli resolving gel.

Immuno-Electron Microscopy

For detection of FPC in mouse cells by immuno-electron microscopy, MEK cells were fixed in freshly prepared 4% formaldehyde/0.1% glutaraldehyde/PBS for 10 min. After thorough washing, the cells were incubated with 803 (1:250) in 0.5% Nonidet P-40/PBS for 1 h, followed by incubation with 10-nm gold-conjugated secondary antibody (1:40; Molecular Probes) for another 1 h. Cells were then postfixed for 1 h in 2.5% glutaraldehyde (electron microscopy grade; Electron Microscopy Services, Washington, PA) in PBS, followed by 1 h in 1% OsO₄ in PBS at room temperature. Cells were washed three times in PBS, dehydrated to 95% ethanol, stained *en bloc* with 4% uranyl acetate in 95% ethanol for 20 min, washed twice with 95% ethanol, and then embedded in Araldite (SPI-Pon Araldite kit; SPI Supplies, West Chester, PA). Thin sections were cut parallel to the surface of the cell monolayer, stained with uranyl acetate and lead citrate, and

examined with a Philips CM10 electron microscope (Philips Medical Systems, Eindhoven, The Netherlands).

Results

Characterization of the Antipeptide Antibodies

The antibodies 803 and 804 were raised in rabbits to a 14-amino acid peptide located in the carboxyl-terminal domain and a 15-amino acid peptide located in the amino-terminal domain of human FPC, respectively, and were then affinity-purified. The former and latter peptides share 50% and 87% amino acid identity, respectively, with the corresponding mouse sequences. With ELISA, both 803 and 804 were observed to bind strongly to their peptides, with titers of more than 1:195,000. To examine the specificity of the antibodies, we generated two *PKHD1* cDNA constructs, *i.e.*, pcDNA4/hPKHD1CT, encoding the entire intracellular tail of the protein, and pcDNA4/hPKHD1NT, encoding part of the extracellular fragment of FPC. Immunoblotting with both 803 and 804 revealed a specific band in HEK 293T cells transiently transfected with the pcDNA4/hPKHD1CT or pcDNA4/hPKHD1NT construct of FPC but not in nontransfected cells or in cells transfected with an empty vector (Figure 1, A1 and B1). The molecular masses of the recombinant proteins (32 and 35 kD) appeared larger than the expected 24 and 27 kD, most likely because of posttranslational modification. To confirm that these bands represented the correct recombinant FPC peptides, we stripped and reblotted the same membranes with a mAb to a Myc tag that was added to the carboxyl-terminal end of the recombinant proteins. The Myc-specific antibody recognized precisely the same bands as 803 and 804 (Figure 1, A2 and B2). Furthermore, the recombinant FPC bands recognized by 803 and 804 could be blocked with preincubation of the antibodies with their respective immunogens (Figure 1, A3 and B3) but not an unrelated peptide (data not shown). The antibody 803 also does not recognize the amino-terminal recombinant protein (Figure 1A4). Collectively, these data demonstrated that 803 and 804 recognize their specific recombinant FPC proteins.

To determine whether 803 and 804 recognized endogenous FPC in human kidney tissues, human renal cortical tubule epithelial cells, and canine MDCK cells, we immunoprecipitated tissue and cell lysates and performed Western blot analyses. The antibody 803 recognized two bands of approximately 450 kD (similar in size to PC1), consistent with two splicing variants of FPC (Figure 1C) (13). In addition, 803 recognized two bands immunoprecipitated from MDCK cells by 804. The weak intensity of the bands likely reflects the relatively low abundance of the FPC protein in these cells.

Detection of FPC in the Primary Cilia and in the Basal Body Area in Human Kidney Tubules

To determine the specificity of 803 in tissue staining, we performed immunostaining with preimmune serum, 803, and 803 plus its immunogen. Because we hypothesized a ciliary localization of FPC, we also double-labeled tissue sections with an antibody to a ciliary marker, acetylated α -tubulin. Whereas the acetylated α -tubulin-specific antibody delineated

the cilia very well, preimmune serum did not yield obvious signals on tissue sections (Figure 2, A to C). Double-labeling with 803 and the acetylated α -tubulin-specific mAb demonstrated that FPC was located primarily in the basal body area,

at the base of the cilium, in collecting duct cells (Figure 2, F to H). The reactivity of 803 with tissue sections was blocked with preincubation with its FPC peptide, whereas staining for acetylated α -tubulin, a ciliary marker, remained (Figure 2, K to M). To confirm that FPC was localized in the peri-basal body region, we double-labeled the cells with 803 and a mAb to γ -tubulin, a basal body marker. We observed that FPC colocalized with γ -tubulin in collecting duct cells (Figure 2, F' to H').

As described above, FPC is located exclusively in the basal body area in human adult kidneys. In human fetal kidneys, we observed a similar pattern of FPC localization at the base of the cilia (data not shown) but we also observed labeling of the shaft of the cilia; FPC completely colocalized with acetylated α -tubulin (Figure 2, P to R). We did not detect specific signals on cilia or in the basal body area (Figure 2, P' to R') in a kidney from a patient with ARPKD.

The immunostaining data for human fetal and ARPKD kidneys were confirmed with 804. Like 803, 804 recognized FPC at the base of the cilia (Figure 3, a to c) and detected no specific signal in a kidney from a patient with ARPKD (Figure 3, a' to c').

FPC Localization to the Primary Cilia and Concentration in Basal Bodies of Mouse Kidney Tubules and Cultured MEK and MDCK Cells

We also stained mouse kidney sections and cultured mouse epithelial cells with 803, to determine whether the FPC expression patterns among human subjects and mice were similar. Preimmune serum did not stain the cilia (Figure 4, A to C). In normal adult mouse kidney, as in human kidney tubules, double-labeling with 803 and acetylated α -tubulin-specific mAb demonstrated that FPC was located mainly in the basal body area in mouse kidney tubules (Figure 4, F to H). The antibody 803 preabsorbed with its peptide failed to stain the basal bodies, whereas acetylated α -tubulin staining was not affected (Figure 4, K to M). To identify a cell line that expresses FPC, we examined FPC expression in embryonic day 15.5 MEK epithelial cells positive for DBA, a collecting duct marker (27). After 2 to 4 d of culture at 33°C, the primary cilium in each cell was visible. Preimmune serum did not demonstrate any stain-

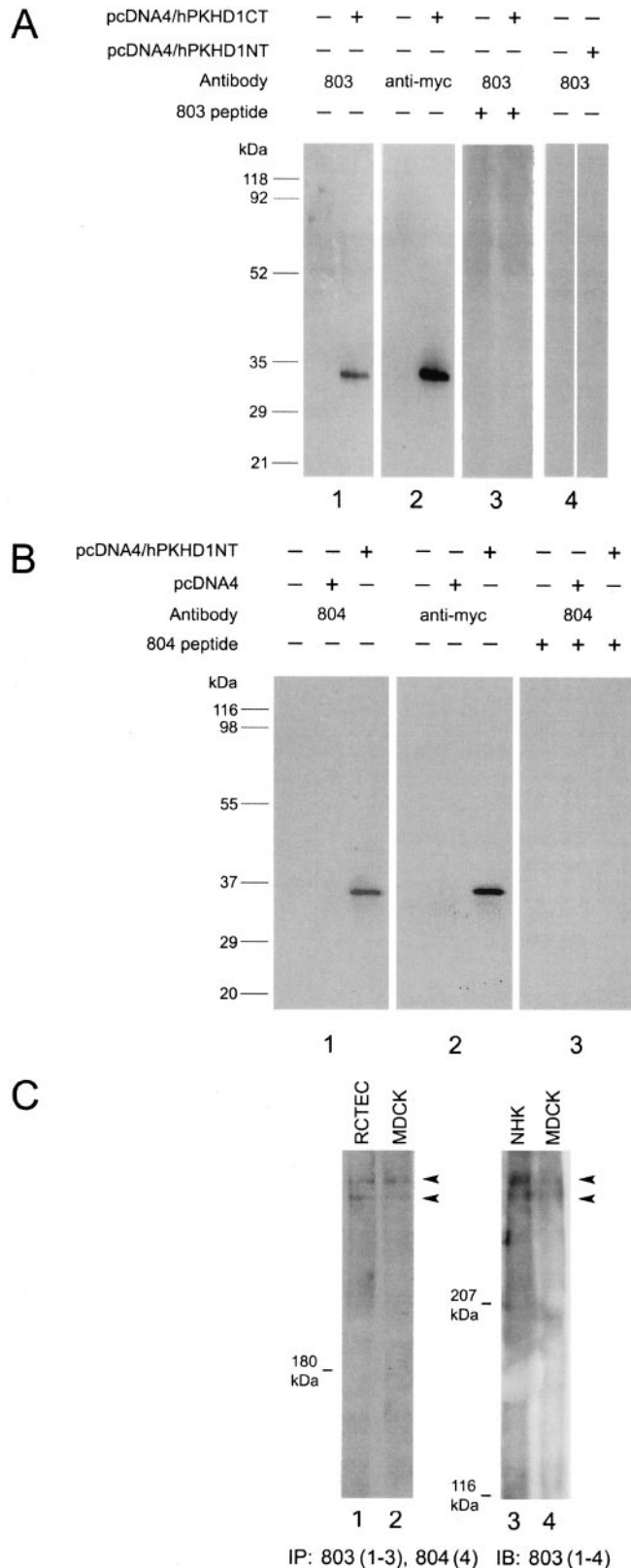


Figure 1. Characterization of fibrocystin/polyductin/tigmin (FPC)-specific antibodies 803 and 804 with Western blot analyses (A and B) and immunoprecipitation (C). Cell lysates of human embryonic kidney (HEK) 293T cells, with or without transfection of pcDNA4/hPKHD1CT or pcDNA4/hPKHD1NT, were blotted with the indicated antibodies; 803 (A) and 804 (B) specifically recognized recombinant FPC (A1 and B1). Empty pcDNA vector was used as a control sample. Bands of the same size also reacted strongly to the Myc tag antibody (A2 and B2). Immunoabsorption of 803 and 804 with the respective FPC peptides totally abolished antibody binding to the recombinant FPC proteins (A3 and B3). The 803 antibody did not cross-react with the Myc tag (A4). The antibodies recognized two large endogenous FPC bands (arrowheads) that were immunoprecipitated from normal human kidney (NHK), human renal cortical tubular epithelial cells (RCTEC), and MDCK cells by 803 and from MDCK cells by 804 (C). IP, immunoprecipitation; IB, immunoblotting.

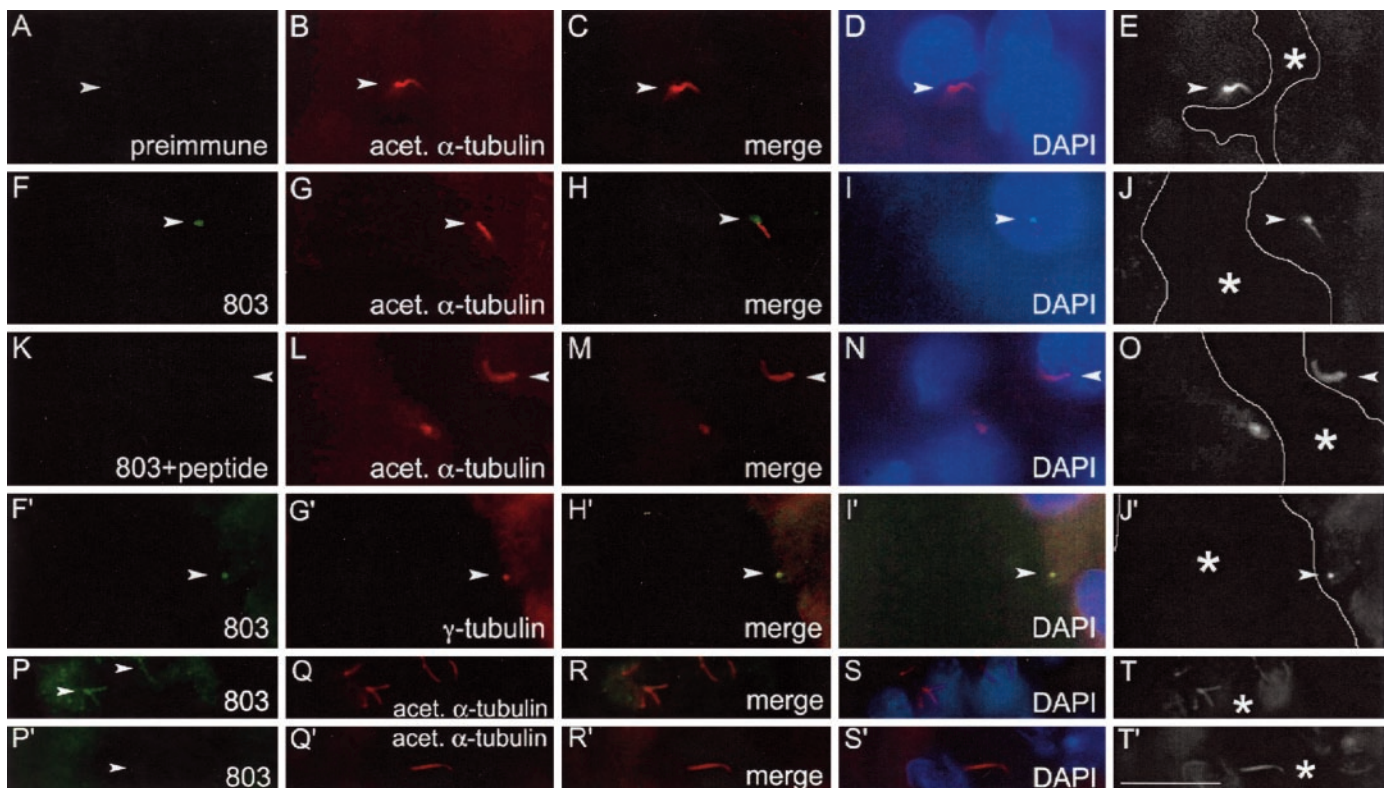


Figure 2. FPC expression in the cilia of human adult and fetal kidney tubules. Double-labeling with 803 (F and F') and mAb to acetylated (acet.) α -tubulin (B, G, and L), a ciliary marker, or mAb to γ -tubulin (G'), a basal body marker, localized FPC to the basal body of the cilium (H and H'). No signal was observed with preimmune 803 serum (A). Preincubation of 803 with its immunogen completely blocked the staining of the cilium (K). In normal human fetal kidney, 803 detected FPC in the ciliary shaft (P), as evidenced by colocalization with acetylated α -tubulin (Q, R). However, no specific signals on cilia or basal bodies were detected in a kidney with autosomal recessive polycystic kidney disease (ARPKD) (P' to R'). Nuclei were stained with 4'-6-diamidino-2-phenylindole (DAPI) (D, I, N, I', S, and S'). In the respective merged images (E, J, O, J', T, and T'), the tubule lumen is indicated (*). C, M, merged image of the left two panels, respectively. Scale bar, 12 μ m.

ing on mouse cells (Figure 5, A to C). Double-labeling with 803 and either α -tubulin-specific or γ -tubulin-specific mAb demonstrated that FPC was clearly situated at the base of the cilium and colocalized with γ -tubulin (Figure 5, E to G and E' to G'). The staining signals for FPC in basal bodies could be blocked with preincubation of 803 with its peptide (Figure 5, I to K). Similar results were obtained when MDCK cells were stained with 803 (Figure 6, A to C).

To confirm our results with 803, we stained MEK cells with 804, which was raised against an amino-terminal epitope of FPC. This antibody also labeled the basal body area, which was identified by double-labeling with γ -tubulin. Interestingly, 804 stained the whole cilium in some cells (Figure 6, m to o). The specificity and staining pattern of 804 were also tested in MDCK cells. Again, FPC was observed in the basal body area (Figure 6, e to g and e' to g') and the ciliary shaft (Figure 6, e'' to g''). Preimmune serum did not yield any staining (Figure 6, a to c). The staining of FPC in primary cilia could be blocked with preincubation of 804 with its FPC peptide (Figure 6, i to k).

FPC Expression in *Pkd1* Mutant Cells

As one way to study the relationship between FPC and PC1, we compared the FPC expression pattern in cells with a targeted *Pkd1*

mutation (*Pkd1*^{null/+}, *Pkd1*^{null/null}, or *Pkd1*^{del34/del34}) with that in wild-type cells. The cells were derived from DBA-positive embryonic day 15.5 MEK specimens from the same litter, with or without a targeted mutation in the mouse *Pkd1* gene (27). We observed that FPC was expressed in the basal bodies and the centrioles of all three kinds of mutant cells (Figure 7, E to G, I to K, and M to O). Neither mislocalization nor a difference in staining intensity was observed among the four groups (Figure 7).

Immuno-Gold Electron-Microscopic Localization of FPC to the Peri-Basal Body Region of Mouse Kidney Cells

To determine whether FPC was located in the basal body itself or was associated with material surrounding the basal body, we performed immuno-gold electron microscopy with 803. Gold particles were associated with fibrous or particulate material adjacent to the basal bodies and centrioles (Figure 8) but were not directly associated with the basal body microtubules themselves or with internal structures of the basal bodies. The particles were frequently observed at the periphery of regions of low electron density surrounding the basal bodies; these regions may represent membrane-bound vesicles whose membranes were disrupted by the permeabilization procedure.

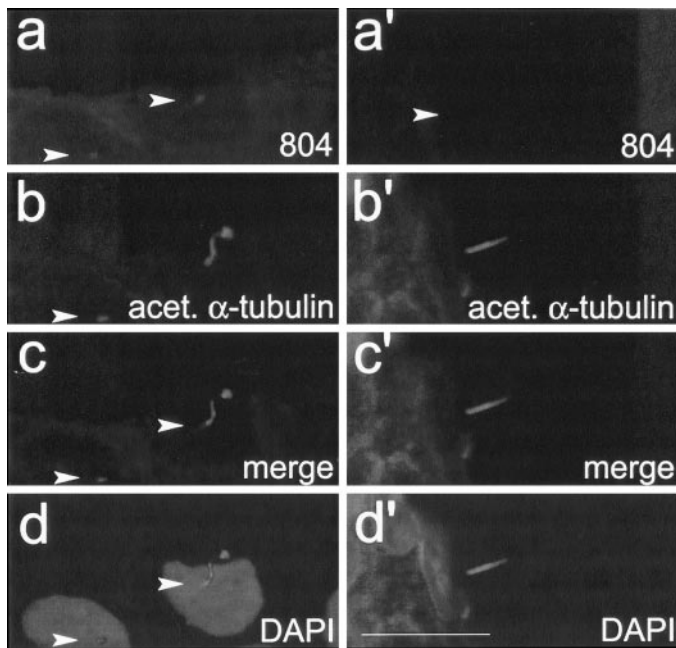


Figure 3. FPC expression recognized by 804 in human fetal and ARPKD kidneys. In normal fetal kidney, 804 localized FPC to the basal body of the cilium (a to c). In a fetal kidney with ARPKD, no specific signal was detected (a' to c'). Nuclei were stained with 4'-6-diamidino-2-phenylindole (DAPI) (d and d'). acet., acetylated. Scale bar, 12 μ m.

Few gold particles were observed in the shaft of the primary cilium or in the cytoplasm further away from the basal bodies.

Discussion

In this study, we examined the subcellular localization of FPC in human and mouse kidney tissues and in cultured mouse and canine kidney cells with two newly generated antibodies,

raised against the carboxyl-terminal and amino-terminal domains of FPC. Our data indicate that FPC is concentrated at ciliary basal bodies/centrioles, with expression in the shafts of some primary cilia. This discovery adds FPC to the growing group of cilium-associated proteins that cause PKD.

The localization pattern observed for FPC is strikingly similar to that previously observed for PC1, a large integral membrane glycoprotein (31–33) that functions in the cilium (27), and for components of the intraflagellar transport (IFT) system, which moves proteins into the cilium and along the ciliary shaft (34). For example, both kinesin II and dynein 1b/2, the motors for anterograde and retrograde IFT, respectively, are located primarily at the base of the cilium, with minor localization to the ciliary shaft (35–37). Similarly, the IFT proteins IFT88/Polaris (25) and IFT52 (37), which are subunits of the IFT particles that carry ciliary proteins as cargo (34), are located primarily in a pool surrounding the basal bodies, with smaller amounts actually engaged in transport along the ciliary shaft. Importantly, defects in the IFT system, specifically in kinesin II (38) and IFT88/Polaris (23), cause structural defects in primary cilia, resulting in cystic kidneys in mice. Immunocytochemical and immuno-electron-microscopic studies cannot distinguish between components of the IFT system and their cargo, which is thought to include membrane proteins (34). However, because FPC is predicted to be a transmembrane protein (12,13), it is likely that its primary localization to the peri-basal body region reflects its presence in post-Golgi vesicles that are targeted to the base of the cilium, where they dock with the plasma membrane before the protein is moved onto the ciliary membrane. Although such membrane vesicles would not be preserved after the standard permeabilization treatment used for immunolocalization, they are readily apparent in specimens prepared for conventional

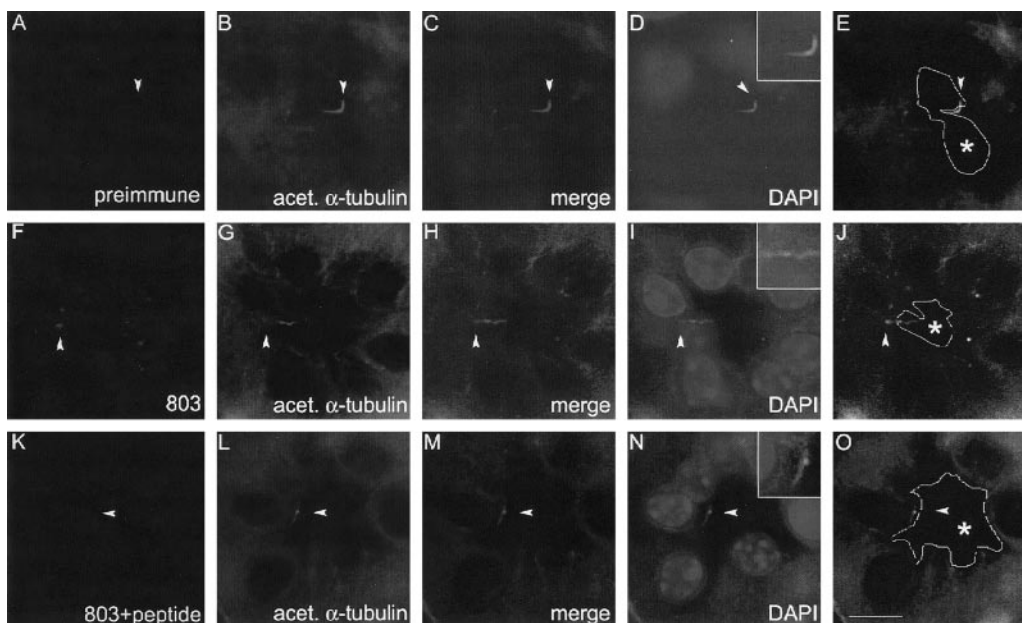


Figure 4. FPC localization to the basal body area of the primary cilium in mouse kidney tubules. No signal was observed with preimmune serum (A). Double-labeling with 803 (F) and mAb to acetylated (acet.) α -tubulin (B, G, and L) localized FPC to the base of the cilium (H). Preincubation of 803 with its immunopeptide blocked the staining in the cilium (K). Cilia are also shown at higher magnification (insets). Nuclei were stained with 4'-6-diamidino-2-phenylindole (DAPI) (D, I, and N). In the respective merged images with black-and-white contrast (E, J, and O), the lumen is indicated (*). C, M, merged image of the left two panels, respectively. Scale bar, 5 μ m.

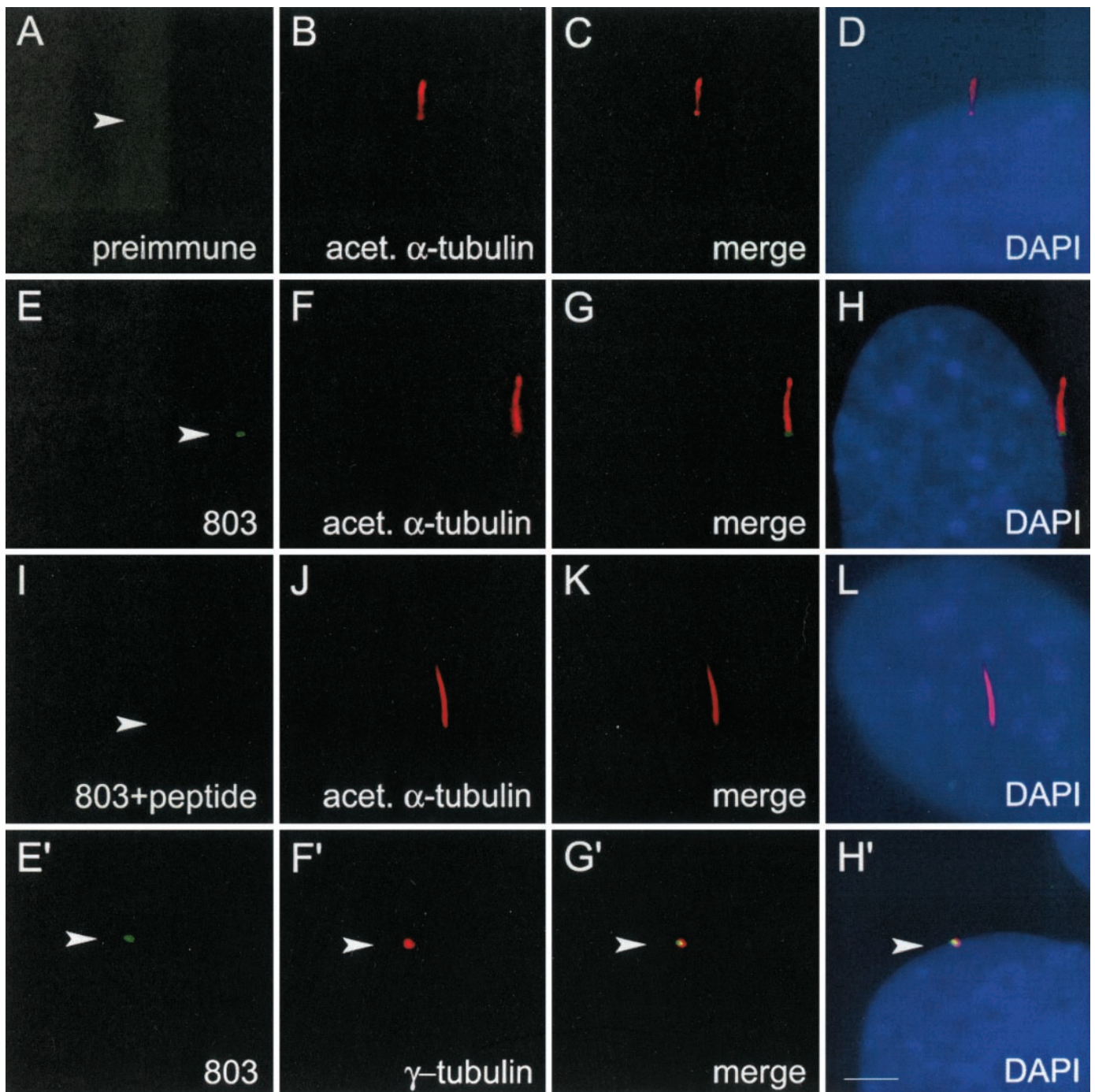


Figure 5. Recognition by 803 of basal bodies in epithelial cells derived from mouse embryonic kidney (MEK). The preimmune serum did not yield any signal in the cells (A). Double-labeling of cultured mouse cells with 803 (E and E') and mAb to acetylated (acet.) α -tubulin (B, F, and J) or γ -tubulin (F') demonstrated that FPC was clearly localized to the basal body of the cilium (E to G and E' to G'). No staining of cilia was observed when 803 was preincubated with its immunopeptide (I). Nuclei were stained with 4'-6-diamidino-2-phenylindole (DAPI) (D, H, L, and H'). C, K, merged image of the left two panels, respectively. Scale bar, 5 μ m.

transmission electron microscopy (39). Similar accumulation and docking of rhodopsin-containing vesicles occur at the base of the mammalian photoreceptor-connecting cilium before fusion of the vesicles with the plasma membrane and transport of rhodopsin, via the connecting cilium, to the photoreceptor outer segment (40). Further studies will be necessary to determine the conditions affecting the relative

amounts of FPC in the peri-basal body region *versus* the ciliary shaft.

The localization of FPC to the basal body region and in some cases the ciliary shaft suggests that FPC has a structural or functional role in the primary cilium. Structural analysis of the FPC molecule indicates that its intracellular domain contains several potential phosphorylation sites for protein kinase A and

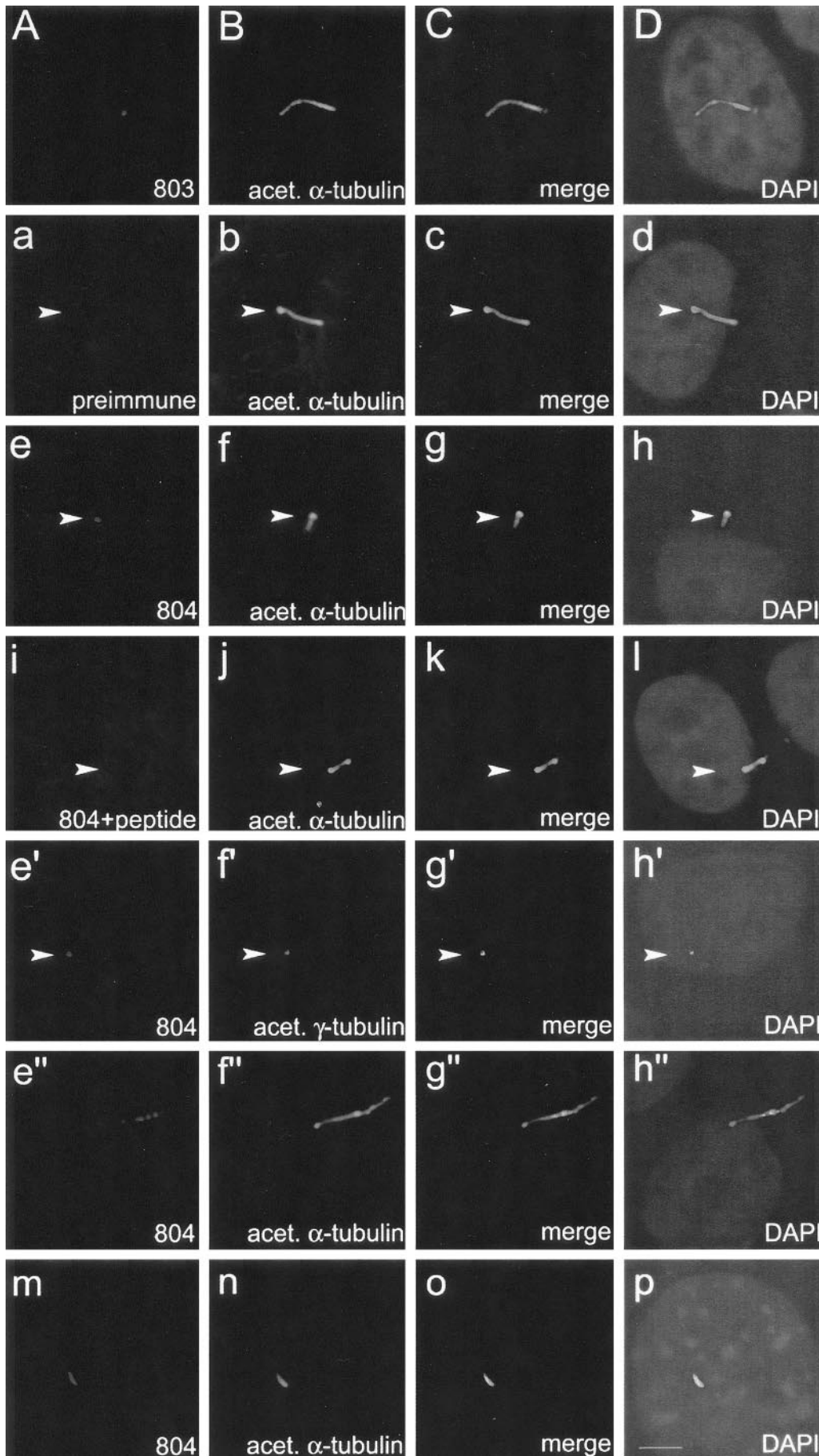


Figure 6. Localization of FPC in MDCK cells and epithelial cells derived from MEK. The antibody 803 localized FPC at the basal body in MDCK cells (A to C). Preimmune 804 serum did not yield any signal in MDCK cells (a). Double-labeling of MDCK cells with 804 (e and e') and mAb to acetylated (acet.) α -tubulin (b, f, j, and f'') or γ -tubulin (f) indicated that FPC was localized to both the basal body and the cilium (e to g and e'' to g''). No staining of cilia was observed when 804 was preincubated with its immunopeptide (i). In mouse cells, FPC was observed on the shaft of the cilia (m to o). Nuclei were stained with 4'-6-diamidino-2-phenylindole (DAPI) (D, d, h, i, h', h'', and p). c, k, and g, merged image of the left two panels, respectively. Scale bar, 5 μ m.

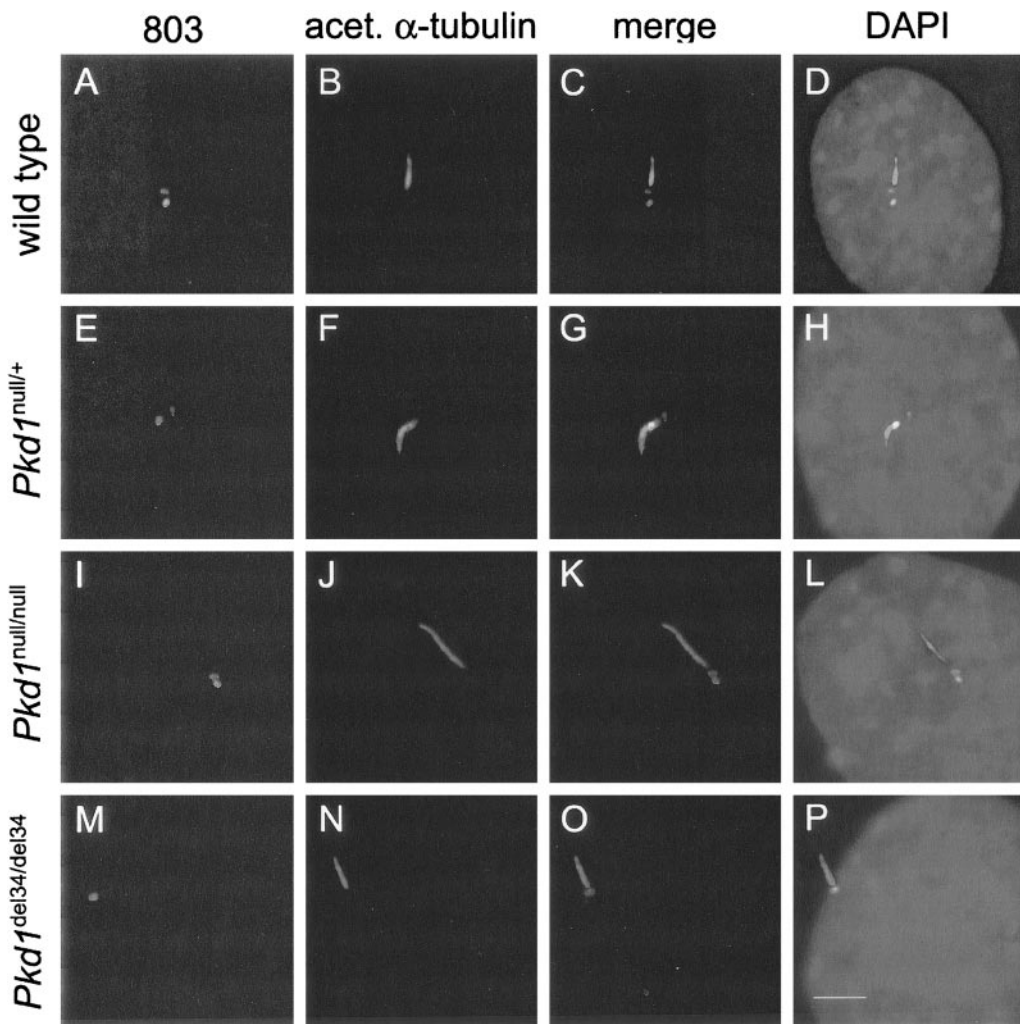


Figure 7. FPC expression in the basal bodies/centrioles in cells with targeted *Pkd1* mutations. In wild-type (A to D), *Pkd1*^{null/+} heterozygous (E to H), *Pkd1*^{null/null} homozygous (I to L), and *Pkd1*^{del34/del34} homozygous (M to P) cells, double-labeling with 803 (A, E, I, and M) and mAb to acetylated (acet.) α -tubulin (B, F, J, and N) revealed that FPC was located exclusively at the basal bodies of cilia and at the centrioles. No obvious difference in localization patterns among cells with different *Pkd1* genotypes was observed (A, E, I, and M). Nuclei were stained with 4'-6-diamidino-2-phenylindole (DAPI) (D, H, L, and P). Scale bar, 5 μ m.

protein kinase C in humans and mice, whereas the extracellular part of the molecule contains several different functional domains, suggesting roles in cellular signaling (12–14). The primary cilium is a sensory organelle that relays signals to the cell body, including those that control cell differentiation, proliferation, and apoptosis (19), and a classic function of the centrosome/basal body is to nucleate or bind microtubules (41,42), thus establishing cell polarity. Therefore, FPC may play a role in transducing extracellular signals to the cell, to control the cell cycle and cell differentiation.

Ciliary length is one parameter for evaluation of the roles of molecules located in the cilium; *e.g.*, the *Tg737^{orp}* mutation in mice causes shorter than normal cilia in kidney tubules (23). We did not observe shorter cilia in *Pkd1*-knockout mice, but we did discover that the *Pkd1* mutant cells failed to initiate Ca^{2+} responses to physiologic fluid flow, indicating that PC1 is a functional component of the cilium (27,43). Considering the similar expression patterns and somewhat similar molecular structures for FPC and PC1, we hypothesize that FPC plays a sensory role in kidney epithelia, as does PC1. It would be interesting to examine the ciliary length in kidney tubules among patients with ARPKD and to test the role of FPC as a mechanosensor.

PKD involves sequential steps from cyst formation and

enlargement to fluid secretion and accumulation within the cysts (44). During this complicated process, abnormal cellular proliferation, differentiation, and/or apoptosis can occur. It is generally thought that cystogenesis results from increased proliferation and de-differentiation, but how *PKHD1* mutations among patients with ARPKD initiate these changes is not known. It is tempting to speculate that FPC interacts with other proteins associated with the basal body/cilium and that its dysfunction results in disruption of the protein complex and leads to cystogenesis. Because the major autosomal dominant PKD protein PC1 is also associated with the basal bodies of primary cilia, we tested the effects of PC1 mutations on FPC expression. We observed no obvious differences in FPC expression levels and patterns between wild-type MEK epithelial cells and cells with various *Pkd1* mutations (*Pkd1*^{null/+}, *Pkd1*^{null/null}, or *Pkd1*^{del34/del34}). Therefore, disruption of PC1 does not seem to physically disrupt the normal localization of FPC, suggesting that FPC localization is independent of the PC1 protein complex. This is consistent with the differences in clinical presentations for patients with ARPKD *versus* autosomal dominant PKD. Further studies are required to determine whether the FPC pathway interacts with the polycystin signaling pathway.

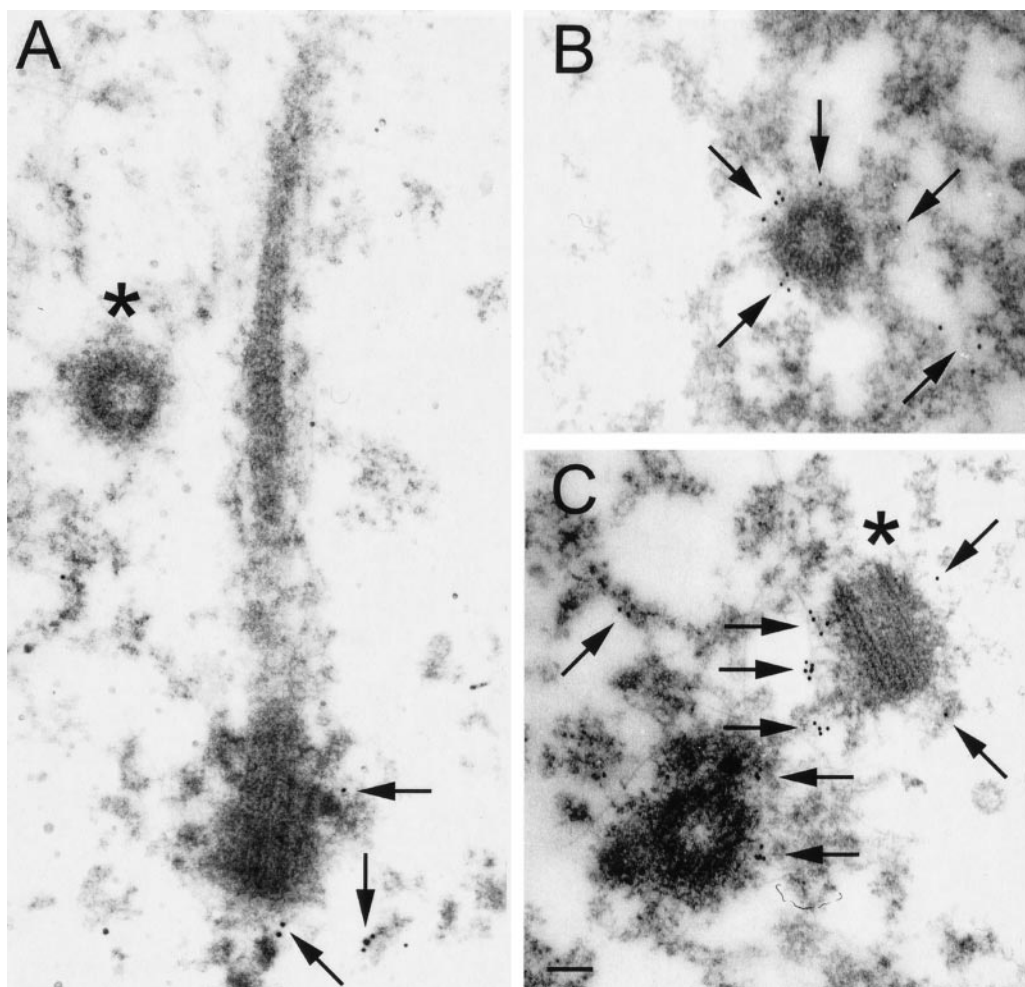


Figure 8. Immunoelectron-microscopic localization of FPC in mouse collecting duct cells. Clusters of gold-conjugated particles (arrows) were observed mainly around the basal body of the primary cilium (A); little or no label was associated with the ciliary shaft or cytoplasm further from the basal body. This cilium is lying parallel to the cell surface; a centriole is marked (*). In cross-sections of basal bodies (B), gold particles (arrows) were observed peripheral to the triplet microtubules; a very similar labeling pattern has been observed for a component of the intraflagellar transport system in the green alga *Chlamydomonas* (37). In some cells (C), gold particles (arrows) were associated with both the basal body and the adjacent centriole (*). Scale bar, 200 nm.

Acknowledgments

We thank Q. Xi and T. Finnerty, in the laboratory of Dr. Zhou, and G. Hendricks, at the University of Massachusetts Medical School Electron Microscopy Facility, for technical support. This work was supported by grants from the National Institutes of Health to Drs. Zhou and Witman. We gratefully acknowledge Diabetes Endocrinology Research Center Grant DK32520, for support of the University of Massachusetts Medical School Electron Microscopy Facility. Dr. Wang is the recipient of a postdoctoral fellowship from the American Heart Association. During revision of this manuscript, an article on FPC localization was published (45), stating that ARPKD protein is located in the plasma membrane and on the cilia in MDCK cells.

References

- Zerres K, Rudnik-Schoneborn S, Steinkamm C, Becker J, Mucher G: Autosomal recessive polycystic kidney disease. *J Mol Med* 76: 303–309, 1998
- Shaikewitz ST, Chapman A: Autosomal recessive polycystic kidney disease: Issues regarding the variability of clinical presentation. *J Am Soc Nephrol* 3: 1858–1862, 1993
- Roy S, Dillon MJ, Trompeter RS, Barratt TM: Autosomal recessive polycystic kidney disease: Long-term outcome of neonatal survivors. *Pediatr Nephrol* 11: 302–306, 1997
- Kaplan BS, Fay J, Shah V, Dillon MJ, Barratt TM: Autosomal recessive polycystic kidney disease. *Pediatr Nephrol* 3: 43–49, 1989
- Kaariainen H, Koskimies O, Norio R: Dominant and recessive polycystic kidney disease in children: Evaluation of clinical features and laboratory data. *Pediatr Nephrol* 2: 296–302, 1988
- Fonck C, Chauveau D, Gagnadoux MF, Pirson Y, Grunfeld JP: Autosomal recessive polycystic kidney disease in adulthood. *Nephrol Dial Transplant* 16: 1648–1652, 2001
- Lieberman E, Salinas-Madrigal L, Gwinn JL, Brennan LP, Fine RN, Landing BH: Infantile polycystic disease of the kidneys and liver: Clinical, pathological and radiological correlations and comparison with congenital hepatic fibrosis. *Medicine (Baltimore)* 50: 277–318, 1971
- Igarashi P, Somlo S: Genetics and pathogenesis of polycystic kidney disease. *J Am Soc Nephrol* 13: 2384–2398, 2002
- Holthofer H, Kumpulainen T, Rapola J: Polycystic disease of the kidney: Evaluation and classification based on nephron segment and cell-type specific markers. *Lab Invest* 62: 363–369, 1990
- Nakanishi K, Sweeney WE Jr, Zerres K, Guay-Woodford LM, Avner ED: Proximal tubular cysts in fetal human autosomal recessive polycystic kidney disease. *J Am Soc Nephrol* 11: 760–763, 2000

11. Bergmann C, Senderek J, Sedlacek B, Pegiazoglou I, Puglia P, Eggermann T, Rudnik-Schneborn S, Furu L, Onuchic LF, De Baca M, Germino GG, Guay-Woodford L, Somlo S, Moser M, Buttner R, Zerres K: Spectrum of mutations in the gene for autosomal recessive polycystic kidney disease (*ARPKD/PKHD1*). *J Am Soc Nephrol* 14: 76–89, 2003
12. Ward CJ, Hogan MC, Rossetti S, Walker D, Sneddon T, Wang X, Kubly V, Cunningham JM, Bacallao R, Ishibashi M, Milliner DS, Torres VE, Harris PC: The gene mutated in autosomal recessive polycystic kidney disease encodes a large, receptor-like protein. *Nat Genet* 30: 259–269, 2002
13. Onuchic LF, Furu L, Nagasawa Y, Hou X, Eggermann T, Ren Z, Bergmann C, Senderek J, Esquivel E, Zeltner R, Rudnik-Schneborn S, Mrug M, Sweeney W, Avner ED, Zerres K, Guay-Woodford LM, Somlo S, Germino GG: *PKHD1*, the polycystic kidney and hepatic disease 1 gene, encodes a novel large protein containing multiple immunoglobulin-like plexin-transcription-factor domains and parallel β -helix 1 repeats. *Am J Hum Genet* 70: 1305–1317, 2002
14. Xiong H, Chen Y, Yi Y, Tsuchiya K, Moeckel G, Cheung J, Liang D, Tham K, Xu X, Chen XZ, Pei Y, Zhao ZJ, Wu G: A novel gene encoding a TIG multiple domain protein is a positional candidate for autosomal recessive polycystic kidney disease. *Genomics* 80: 96–104, 2002
15. Nagasawa Y, Matthiesen S, Onuchic LF, Hou X, Bergmann C, Esquivel E, Senderek J, Ren Z, Zeltner R, Furu L, Avner E, Moser M, Somlo S, Guay-Woodford L, Buttner R, Zerres K, Germino GG: Identification and characterization of *Pkhd1*, the mouse orthologue of the human *ARPKD* gene. *J Am Soc Nephrol* 13: 2246–2258, 2002
16. Srinivas S, Goldberg MR, Watanabe T, D'Agati V, Al-Awqati Q, Costantini F: Expression of green fluorescent protein in the ureteric bud of transgenic mice: A new tool for the analysis of ureteric bud morphogenesis. *Dev Genet* 24: 241–251, 1999
17. Lubarsky B, Krasnow MA: Tube morphogenesis: Making and shaping biological tubes. *Cell* 12: 19–28, 2003
18. Ong AC, Wheatley DN: Polycystic kidney disease: The ciliary connection. *Lancet* 361: 774–776, 2003
19. Pazour GJ, Witman GB: The vertebrate primary cilium is a sensory organelle. *Curr Opin Cell Biol* 15: 105–110, 2003
20. Beisson J, Wright M: Basal body/centriole assembly and continuity. *Curr Opin Cell Biol* 15: 96–104, 2003
21. Flood PR, Totland GK: Substructure of solitary cilia in mouse kidney. *Cell Tissue Res* 183: 281–290, 1977
22. Roth KE, Rieder CL, Bowser SS: Flexible-substratum technique for viewing cells from the side: Some *in vivo* properties of primary (9+0) cilia in cultured kidney epithelia. *J Cell Sci* 89: 457–466, 1988
23. Pazour GJ, Dickert BL, Vucica Y, Seeley ES, Rosenbaum JL, Witman GB, Cole DG: *Chlamydomonas IFT88* and its mouse homologue, polycystic kidney disease gene *tg737*, are required for assembly of cilia and flagella. *J Cell Biol* 151: 709–718, 2000
24. Qin H, Rosenbaum JL, Barr MM: An autosomal recessive polycystic kidney disease gene homolog is involved in intraflagellar transport in *C. elegans* ciliated sensory neurons. *Curr Biol* 11: 457–461, 2001
25. Taulman PD, Haycraft CJ, Balkovetz DF, Yoder BK: Polaris, a protein involved in left-right axis patterning, localizes to basal bodies and cilia. *Mol Biol Cell* 12: 589–599, 2001
26. Praetorius HA, Spring KR: Bending the MDCK cell primary cilium increases intracellular calcium. *J Membr Biol* 184: 71–79, 2001
27. Nauli SM, Alenghat FJ, Luo Y, Williams E, Vassilev P, Li X, Elia AE, Lu W, Brown EM, Quinn SJ, Ingber DE, Zhou J: Polycystins 1 and 2 mediate mechanosensation in the primary cilium of kidney cells. *Nat Genet* 33: 129–137, 2003
28. Lu W, Peissl B, Babakhanlou H, Pavlova A, Geng L, Fan X, Larson C, Brent G, Zhou J: Perinatal lethality with kidney and pancreas defects in mice with a targeted *Pkd1* mutation. *Nat Genet* 17: 179–181, 1997
29. Lu W, Fan X, Basora N, Babakhanlou H, Law T, Rifai N, Harris PC, Perez-Atayde AR, Rennke HG, Zhou J: Late onset of renal and hepatic cysts in *Pkd1*-targeted heterozygotes. *Nat Genet* 21: 160–161, 1999
30. Loghman-Adham M, Nauli SM, Soto CE, Kariuki B, Zhou J: Immortalized epithelial cells from human autosomal dominant polycystic kidney cysts. *Am J Physiol* 285: F397–F412, 2003
31. International Polycystic Kidney Disease Consortium: Polycystic kidney disease: The complete structure of the *PKDI* gene and its protein. *Cell* 81: 289–298, 1995
32. Hughes J, Ward CJ, Peral B, Aspinwall R, Clark K, San Millan JL, Gamble V, Harris PC: The polycystic kidney disease 1 (*PKDI*) gene encodes a novel protein with multiple cell recognition domains. *Nat Genet* 10: 151–160, 1995
33. Ponting CP, Hofmann K, Bork P: A latrophilin/CL-1-like GPS domain in polycystin-1. *Curr Biol* 9: R585–R588, 1999
34. Rosenbaum JL, Witman GB: Intraflagellar transport. *Nat Rev Mol Cell Biol* 3: 813–825, 2002
35. Cole DG, Diener DR, Himelblau AL, Beech PL, Fuster JC, Rosenbaum JL: *Chlamydomonas* kinesin-II-dependent intraflagellar transport (IFT): IFT particles contain proteins required for ciliary assembly in *Caenorhabditis elegans* sensory neurons. *J Cell Biol* 141: 993–1008, 1998
36. Pazour GJ, Dickert BL, Witman GB: The DHC1b (DHC2) isoform of cytoplasmic dynein is required for flagellar assembly. *J Cell Biol* 144: 473–481, 1999
37. Deane JA, Cole DG, Seeley ES, Diener DR, Rosenbaum JL: Localization of intraflagellar transport protein IFT52 identifies basal body transitional fibers as the docking site for IFT particles. *Curr Biol* 11: 1586–1590, 2001
38. Lin F, Hiesberger T, Cordes K, Sinclair AM, Goldstein LS, Somlo S, Igarashi P: Kidney-specific inactivation of the KIF3A subunit of kinesin-II inhibits renal ciliogenesis and produces polycystic kidney disease. *Proc Natl Acad Sci USA* 100: 5286–5291, 2003
39. Weber WA, Lee J: Fine structure of mammalian renal cilia. *Anat Rec* 182: 339–344, 1975
40. Deretic D, Papermaster DS: Polarized sorting of rhodopsin on post-Golgi membranes in frog retinal photoreceptor cells. *J Cell Biol* 113: 1281–1293, 1991
41. Lange BM: Integration of the centrosome in cell cycle control, stress response and signal transduction pathways. *Curr Opin Cell Biol* 14: 35–43, 2002
42. Preble AM, Giddings TM Jr, Dutcher SK: Basal bodies and centrioles: Their function and structure. *Curr Top Dev Biol* 49: 207–233, 2000
43. Luo Y, Vassilev PM, Li X, Kawanabe Y, Zhou J: Native polycystin 2 functions as a plasma membrane Ca^{2+} -permeable cation channel in renal epithelia. *Mol Cell Biol* 23: 2600–2607, 2003
44. Sullivan LP, Wallace DP, Grantham JJ: Epithelial transport in polycystic kidney disease. *Physiol Rev* 78: 1165–1191, 1998
45. Ward CJ, Yuan D, Masyuk TV, Wang X, Punyashthiti R, Whelan S, Bacallao R, Torra R, LaRusso NF, Torres VE, Harris PC: Cellular and subcellular localization of the *ARPKD* protein: Fibrocystin is expressed on primary cilia. *Hum Mol Genet* 12: 2703–2710, 2003.